Δελτίο της Ελληνικής Γεωλογικής Εταιρίας, 2010
Πρακτικά 12ου Διεθνούς Συνεδρίου
Πάτρα, Μάιος 2010

Bulletin of the Geological Society of Greece, 2010
Proceedings of the 12th International Congress
Patras, May, 2010

INTERMEDIATE TERM EARTHQUAKE PREDICTION BASED ON INTEREVENT TIMES OF MAINSHOCKS AND ON SEISMIC TRIGGERING

Papazachos B.C., Karakaisis G.F., Papazachos C.B. and Scordilis E.M.

Department of Geophysics, School of Geology, Faculty of Science, Aristotle University, GR54124, Thessaloniki, GREECE, karakais@geo.auth.gr, kpapaza@geo.auth.gr, manolis@geo.auth.gr

Abstract

Two models, which contribute to the knowledge on intermediate term earthquake prediction are further examined, improved and applied. The first of these models, called Time and Magnitude Predictable (TIMAP) regional model is based on repeat times of mainshocks generated by tectonic loading on a network of faults which are located in a certain seismic region (faults' region). The second model, called Decelerating-Accelerating Strain (D-AS) model, is based on triggering of a mainshock by its preshocks.

Parameters of the TIMAP model have been specified for the Aegean area and applied by a backward test in 86 circular faults' regions of this area. The test shows the validity of this time dependent model with 29% false alarms.

Data concerning decelerating and accelerating seismic (Benioff) strain, which preceded 46 strong (M≥6.3) recent mainshocks in a variety of global seismotectonic regimes, show that the generation of a mainshock is triggered by quasi-static stress changes due to accelerating preshocks which occur in a broad (critical) region and by static stress changes due to the large number (frequency of occurrence) of small preshocks generated in a narrow (seismogenic) region. Retrospective predictions (postdictions) of these 46 mainshocks by the D–AS model confirms previous results concerning the prediction uncertainties (2σ) of the model in the origin time (± 2.5 years), epicenter location (≤ 150 km) and magnitude (± 0.4) of an ensuing mainshock with a probability ~ 80%. Information is also given on the successful prediction by the D-AS model of: 1) the Cythera strong (M = 6.9) earthquake which occurred on 8 January 2006 in the southwestern part of the Hellenic Arc and 2) of the Rhodes strong (M = 6.4) earthquake which occurred on 15 July 2008 in the Eastern part of this Arc.

A backward combined application of both models in the Aegean area shows an uncertainty ≤120km in the epicenter location of an ensuing mainshock.

1. Introduction

Seismic hazard assessment currently applied is mainly based on the spatial distribution of the mean seismicity because knowledge of the time variation of seismicity is considered insufficient for such practical application. This is due to the fact that prediction of individual strong earthquakes, which are those that cause damage, is a very difficult scientific problem. The solution of this problem can contribute significantly to the development of techniques for time dependent seismic hazard assessment. For this reason prediction of individual strong earthquakes is one of the most important problems of seismology from the social point of view.

Decades of research work on short term prediction (time uncertainty of days to weeks) led to the conclusion that such prediction is not possible with the present scientific knowledge (Wyss, 1997). Long – term earthquake prediction (uncertainty of the order of decades) is also not possible. This is due to the fact that the physical process of generation of a strong earthquake in a fault is characterized by properties of deterministic chaos that require very accurate knowledge of this process in order to predict the next strong earthquake in the fault (Jaumé and Sykes, 1999). Obtaining such knowledge is also not feasible at present. It seams, however, that there is much hope for intermediate-term earthquake prediction (uncertainty of the order of a few years) by the use of seismological observations related to: a) the time variation of stress due to tectonic loading (repeat times of mainshocks, etc) and b) seismic triggering due to precursory stress fluctuations (precursory change of seismicity).

Time variation of stress due to both physical causes (tectonic loading, triggering) has been considered for improving knowledge on earthquake prediction because both contribute to earthquake generation. Thus, long-wavelength stresses associated with the relative motion of major tectonic plates accumulate relatively slowly (~ 10^{-5} MPa per year) while typical frictional strength of seismic faults is relatively high (1 to 10 MPa) (Hill and Prejean, 2006). For this reason, regional stress may remain below the frictional strength of faults for a long time. Therefore, short–term and short–wavelength fluctuations in both the stress field and fault strength are needed in order the local stress state to exceed local failure threshold and contribute to earthquake generation. That is, in addition to tectonic loading, some kind of triggering mechanism is necessary to explain generation of strong earthquakes. Sources of short-term stress fluctuations can be other earthquakes in the crust (Freed, 2005; Steacy et al., 2005), other physical factors (magmatic intrusions, earth's tides, etc) and anthropogenic activities (reservoir filling, etc). Local fluctuation of fault strength results usually from changes in the fluid pore pressure within the fault.

Quantitative information on tectonic loading can be obtained by using data from several sources (seismological, geological, geodetic, etc) but for seismological purposes (seismicity, seismic hazard, earthquake prediction) seismological data (instrumental, historic) are the most proper ones because such data give direct information on the seismic effect of tectonic loading and are easily quantified. Seismological data useful for improving knowledge on earthquake prediction can be the repeat times of large earthquakes (Fedotov, 1965; Shimazaki and Nakata, 1980). There is, however, a limited number of strong earthquakes which occurred on a particular seismic fault for which quantitative information (size, origin time) is available for reliable statistical treatment. For this reason, a seismic region, which includes "a network of neighboring seismic faults" must be considered to increase available repeat times. On this idea it is based the "Time and Magnitude Predictable Regional" model (Papazachos, 1989; Papazachos et al., 1997) in which a large sample of interevent times of strong earthquakes is available in the region for a reliable study of time dependent seismicity.

Stress change in the focal region of a triggering earthquake is transferred in the focal region of a triggered earthquake in three main modes: the static, quasi-static and dynamic.

Static stress change is the perturbation of the static stress field from just before an earthquake to shortly after the generation of seismic waves by elastic dislocation models (Das and Scholz, 1981; King and Cocco, 2001). Static stress changes decay relatively rapidly with distance, Δ, from the epicenter of the triggering earthquake (as Δ^{-3}) and for this reason their triggering potential is limited to one or two source dimensions from the focus of the triggering earthquake.

Quasi-static stress change is the gradual stress perturbations caused by the viscous relaxation of the plastic lower crust and upper mantle in response to the sudden generation of the triggering earthquake across the fault in the overlying brittle crust (Pollitz and Sacks, 2002). Quasi-static stress changes propagate as a two dimensional stress change and thus decays more slowly with distance (as

~Δ^{-2}) and their triggering potential extends to greater distances than static stress changes. On the other hand, the relatively low speed of viscoelastic propagation results in delayed triggering. Both static and quasi-static stress transfer cause permanent stress change in the vicinity of the fault of the triggered earthquake, which shifts the stress state incrementally to the Coulomb failure threshold on the fault.

Dynamic stress propagates as seismic waves and for this reason its amplitude decreases relatively slowly with distance (as Δ^{-2} for body waves and $\Delta^{-3/2}$ for surface waves) and their triggering potential extends from near field to much greater distances than static or quasi-static stress changes (Kilb et al., 2002). Dynamic triggering potential can be further enhanced by amplification of radiation directivity or by stimulating aseismic process (creep, fluid activation) which contribute to triggered seismicity. Dynamic stress is oscillatory and for this reason leaves no permanent stress to overcome Coulomb failure stress in a fault.

Fluctuation of stress is expressed by corresponding deviations of seismicity from the background one caused by tectonic loading. Such seismicity deviations can be positive (seismic excitation) or negative (seismic quiescence). Several precursory seismicity patterns based on such seismicity deviations have been proposed for improving knowledge on earthquake prediction. One of the most distinct such patterns is formed of a precursory seismic excitation in a broad region and of reduced seismicity in the narrow focal region of an ensuing mainshock, originally proposed by Mogi (1969) who called it "doughnut pattern".

Significant additional research by several workers has shown that seismic excitation in the broad (critical) region is characterized by an accelerating generation of intermediate magnitude preshocks (Tocher, 1959; Varnes, 1989; Sykes and Jaumé, 1990; Knopoff et al., 1996; Brehm and Braile, 1998, 1999; Papazachos and Papazachos, 2000, 2001; Robinson, 2000; Tzanis et al., 2000; Tzanis and Makropoulos, 2002; Ben-Zion and Lyakhovsky, 2002; Scordilis et al., 2004; Papazachos et al., 2005b; Mignan et al., 2006, among others). Bufe and Varnes (1993) have shown that the cumulative Benioff strain (sum of square root of seismic energy), S(t), for the accelerating pattern is expressed by relations of the form:

$$S(t) = A + B(t_c - t)^m \tag{1}$$

where t_c is the origin time of the mainshock and A, B, m parameters calculated by the available data with m<1 and B negative.

Intermediate – term quiescence of seismicity of small shocks in the focal region has been also observed before many strong earthquakes and was attributed to stress relaxation due to aseismic sliding (Wyss et al., 1981; Kato et al., 1997). Some researchers (Evison and Rhodes, 1997; Rhoades and Evison, 1993; Evison, 2001) have observed that a seismic excitation phase can be found in the narrow (seismogenic) region preceding seismic quiescence. Papazachos et al. (2005a) used global data to show that intermediate magnitude preshocks in the seismogenic region form a decelerating pattern and the time variation of the cumulative Benioff strain up to the mainshock also follows a power–law (relation 1) but with a power value larger than one (m>1). That is, this pattern of decelerating strain in the focal (seismogenic) region is formed of a transient excitation, followed by a decrease of seismicity of intermediate magnitude shocks.

Papazachos et al. (2006), taking into consideration the above mentioned published information on the observed accelerating and decelerating precursory seismicity and based on such seismicity which preceded globally occurred strong mainshocks (M≥6.0) developed the Decelerating-Accelerating Strain (D-AS) model for intermediate term earthquake prediction. This model is based on empirical relations and parameters most of which have been also derived theoretically and can be physically interpreted.

These constraints relate parameters of a decelerating and an accelerating preshock sequence with the main parameters (origin time, magnitude, epicenter geographic coordinates) of the ensuing mainshock, hence they can, in principle, be used to perform intermediate term prediction of mainshocks.

A goal of the present work is to further develop the time and magnitude predictable (TIMAP) regional model by performing a backward test of this model on strong (M≥6.0) shallow (h≤100km) mainshocks generated in circular faults' regions of the Aegean area (34^0N-43^0N, 19^0E-30^0E). Another goal is to further study properties of the space, time and magnitude distributions of already occurred decelerating and accelerating preshock sequences of 46 recently occurred (since 1980) strong (M≥6.3) shallow (h≤100km) mainshocks in a variety of global seismotectonic regimes. We also show how these properties have been used to form the Decelerating-Accelerating Strain (D-AS) model which is applied in a backward test to estimate its time, space and magnitude uncertainties. Properties of preshocks are also used to give reasonable physical explanations for triggering of a mainshock by its preshocks.

2. The Time and Magnitude Predictable (TIMAP) Model

The TIMAP model is based on the interevent times of mainshocks generated on a network of faults which are located in a seismic region (faults' region). That is, the original catalogue of the region is declustered so that preshocks which trigger a mainshock and postshocks which are triggered by the mainshock are excluded. Thus, seismic triggering is removed and the finally employed catalogue includes only mainshocks caused mainly by tectonic loading. Also, the interevent time considered in this model is the time between mainshocks generated in different faults of the region.

Papazachos et al. (1997) used a large sample of global data (1811 interevent times of mainshocks which occurred in 274 regions located in different seismotectonic regimes) to define the relations:

$$\log T_t = 0.19M_{\min} + 0.33M_p + Q \tag{2}$$

$$M_f = 0.73M_{\min} - 0.28M_p + W \tag{3}$$

where T_t (in years) is the interevent time, M_{min} is the minimum mainshock magnitude considered, M_p is the magnitude of the previous mainshock in the seismic region and M_f is the magnitude of the following mainshock in the region. Q and W are constants which depend on the long-term seismicity level of the seismic region and their mean values (as well as their standard deviation σ_q and σ_w) are calculated by the available data for each region.

Relations (2) and (3) have been derived by using a moment magnitude based on the total seismic moment released by the mainshock and its preshocks and postshocks. This is also done in the present work to calculate Q and W by considering as preshocks and postshocks those events which occurred in a time window ±8.5 years from the origin time of the mainshock. It must be noticed, however, that the differences between the mainshock magnitudes calculated in this way and the observed ones are within the errors' window.

It has been further shown (Papazachos and Papaioannou, 1993; Papazachos et al., 1997) that the ratio T/T_t of the observed interevent time, T, to the calculated, T_t, by relation (2) follows a lognormal distribution, with a mean value equal to zero and a standard deviation, σ_q, which varies from region to region. It means that we can calculate the probability, P, for the occurrence of a mainshock with $M \geq M_{min}$ during the next Δt years, when the previous such mainshock ($M_p \geq M_{min}$) occurred t

years ago, by the relation:

$$P(\Delta t) = \frac{F\left(L_2/\sigma\right) - F\left(L_1/\sigma\right)}{1 - F\left(L_1/\sigma\right)} \tag{4}$$

where, $L_2 = \log\frac{t+\Delta t}{T_t}$, $L_1 = \log\frac{t}{T_t}$ and F is the complementary cumulative value of the normal distribution with mean equal to zero and standard deviation, $\sigma(=\sigma_q)$, where $\sigma_q(=0.15)$ is the average value of the standard deviations calculated for 218 regions in the Aegean area. T_t is calculated by relation (2) since M_{min}, M_p and Q are known.

2.1 Application of the TIMAP model in the Aegean area

Karakaisis et al., (2010) used the catalogue of instrumental (M≥5.2, 1911-2008, h≤100km) data (Papazachos et al., 2008) and of historical (M≥6.0, 464BC-1910) data (Papazachos and Papazachou, 2003) for earthquakes in the Aegean area (34^0N-43^0N, 19^0E-30^0E) to define circular focal regions, (C,r). Center, C, of a circular region is the epicenter of the largest known earthquake ever occurred with this epicenter and with magnitude M_{max} (≥6.0). The radius r (= L/2) is equal to the half fault length of this largest earthquake. For the whole Aegean area (Aegean sea and surrounding lands) 223 such circular focal regions have been defined. Karakaisis and his colleagues (2010) also developed and applied a declustering procedure to exclude associated shocks (preshocks, postshocks) that occurred in the focal region and in a time window ±8.5 years from the origin time of each mainshock. The mainshocks (with M≥5.2) have been identified in each circular focal region and a catalogue of mainshocks has been formed for the whole Aegean area. Furthermore, they defined completeness of mainshocks in each circular region (C, R = 100km). Thus, in each of the 223 such circular regions there is available not only the complete sample of instrumental data (M≥5.2, 1911-2008) but corresponding complete samples of historical mainshocks too.

These complete samples of mainshocks in each of the 223 circular regions of the Aegean area are used in the present work to define 218 circular (C, R≤100km) regions where the TIMAP model holds. For these regions there are calculated the constants Q and W of relations (2) and (3) and the corresponding standard deviations, σ_q and σ_w. A backward test of the model is applied for 86 of these circular regions which include the epicenters of the last two mainshocks with M≥6.0 and the latest (target mainshock) is different in these 86 cases and is retrospectively predicted, as it is explained in the following.

The values of the scaling coefficients (b = 0.19, c = 0.33) of relation (2) and (B = 0.73, C = -0.28) of relation (3) have been calculated by the use of a very large sample of global data, while the corresponding sample for the Aegean area is much smaller. For this reason, the global values of these scaling coefficients are adopted for the Aegean area too. To further support this approach the following test was also performed: By using a sample of 161 interevent times of mainshocks in the Aegean area with a constant M_{min} = 6.0±0.2 (where ±0.2 is the error window) a mean value c^* = 0.47 was determined for the scaling coefficient of the relation $logT_t = c^*M_p + Q$. On the other hand, c^* for the global data is approximately equal to $b+c$ = 0.52, which is in good agreement with the value determined by data in Aegean. This supports the adoption of the scaling coefficients of relation (2), which is the most important one of the TIMAP model.

For each of the 218 centers, C, circles are defined, (C, R), with $R_1 \le R \le R_2$ and a step δR (e.g. R_1 =

20km, R_2 = 100km, δR = 5km). Then, relation (2) is applied to calculate the constant Q by using all available sets ($M_{min} \geq 5.2$, M_p, $logT_t$) in each such circle. As best solution we considered that one for the circle (C, R_σ) for which the number, N_σ, of sets (interevent times) is larger than a certain value, $N_\sigma \geq N_{min}$ (e.g. N_{min} = 4), and the standard deviation, σ_q, takes its smallest value (σ_q = minimum). For each of these regions the values of R_σ and N_σ, the average value of Q and the corresponding standard deviation, σ_q, are determined. Also, the available sets ($M_{min} \geq 5.2$, M_p, M_f) of data for each of the circular regions have been used to define a circle (C, $R_w \leq 100$km) for which the standard deviation takes its smallest value. The complete mainshock data for this circle are used to define the average value of W of relation (3) for each circular region, with a standard deviation σ_w. The average values of the standard deviations for all 218 regions are $\sigma_q = 0.15 \pm 0.06$ and $\sigma_w = 0.21 \pm 0.08$.

A backward test of the TIMAP model is performed to examine its prediction potentiality, that is, to get an idea about the range of uncertainties of the retrospectively predicted by this model epicenters and magnitudes of strong ($M \geq 6.0$) mainshocks. For this purpose, a "target mainshock" is retrospectively predicted on the basis: of the parameters of a previous known mainshock (location, origin time, magnitude) and of known parameters (C, R_σ, Q, σ_q, R_w, W, σ_w) of circular faults' regions where the epicenters of both mainshocks are located. There are 86 such circular seismic regions in the Aegean area which include at least two strong ($M \geq 6.0$) mainshocks with different last mainshocks. These 86 last mainshocks are taken as "target mainshocks" which have been estimated (predicted) retrospectively.

Such retrospective predictions have been made for each one of the 86 target mainshocks. Usually more than one faults' centers, $C(\phi,\lambda)$, are clustered near the epicenter of the mainshock. Thus, the predicted epicenter, $E_t(\phi,\lambda)$, is the geographic mean of the clustered centers, $C(\phi,\lambda)$. In particular, the backward test shows that the distance between the epicenter, E_t, defined by the TIMAP model and the observed epicenter, E, is given by the relation $(EE_t) = 90 \pm 40km$, where $40km$ is one standard deviation, σ. This backward test also shows that the magnitude predicted by the TIMAP model, M_t, for each center, $C(\phi,\lambda)$, is equal to $M_f+0.3$ for $M_f \leq 6.4$, to $M_f+0.2$ for M_f between 6.5 and 6.9 and to $M_f+0.1$ for $M_f \geq 7.0$, where M_f is given by the relation (3). In case of clustered centers, the adopted magnitude is the average of the M_t magnitudes calculated for each center of the cluster. The uncertainty of the magnitude M_t estimated this way is $\sigma = 0.21$. Figure (1) shows the cumulative frequency distribution of the probabilities P_t (Δt = 10years) defined by the TIMAP model on the basis of the available data 2 years before the generation of the 86 target mainshocks with $M \geq 6.0$, of the 66 mainshocks with $M \geq 6.5$ and of the 38 mainshocks with $M \geq 7.0$.

A backward test has been also performed to define the percentage of false alarms. For this purpose, it has been attempted a retrospective prediction of the strong ($M \geq 6.0$) mainshocks which occurred in the whole Aegean area during the time period 1981-2008 when a dense network of seismographic stations has been in operation in this area. The test is based on these data of strong mainshocks and on the 218 circular faults' regions (C, R$\leq$100km) in which the epicenters of corresponding mainshocks are located. The test is also based on the observation that the rate of mainshocks with M$\geq$6.0 in the whole Aegean area is r = 12.6 (with σ = 2.6) earthquakes per decade during the period 1966-2008 when networks of seismic stations were in operation in Greece. That is, the maximum number of expected mainshocks per decade is r+2σ = 18.

The TIMAP model has been applied separately for each one of the nineteen decades, 1981-1990, 1982-1991, …, 1999-2008 and for each of the 218 circular faults' regions. Probabilities, P_t(δt = 10years) have been calculated using relations (2) and (4) with σ = 0.15, which is the average of the calculated σ_q values and by selecting the highest P_t from its values calculated for M_{min} equal to 6.0, 6.5 and 7.0.

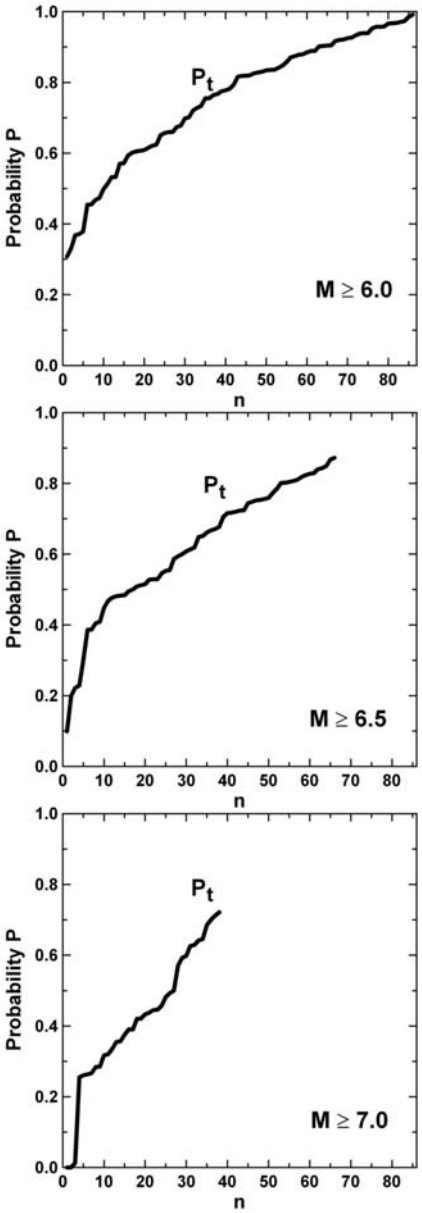

Fig. 1: The probability P(Δt = 10years), as a function of the cumulative frequency, n, of occurrence for the generation of a strong mainshock (M≥6.0 upper part, M≥6.5 middle part and M≥7.0 lower part) in circular faults' regions (C, R≤100km) of the Aegean sea and surrounding lands. Distribution of Pt comes from calculations based on the time dependent (TIMAP) model for a 10 years period which started two years before the generation of each one of the already occurred strong mainshocks.

Thus, for each decade a probability was calculated for each one of the 218 circular faults' regions. Of those, the 18 regions with the eighteen highest probabilities were considered and their locations in respect to the epicenters of the mainshocks occurred in this decade were examined. A faults' re-

gion is considered as "predicting" if it includes the epicenter of at least one strong ($M \geq 6.0$) mainshock of the decade, otherwise the region is considered as "false alarming". This procedure has been repeated for each one of the nineteen decades.

The result of this test is that 243 of the examined regions have been characterized as predicting and 99 as false alarming, that is, the false alarming percentage is 29% for the TIMAP model in the Aegean area. This percentage can be attributed to the non strong triggering of these faults' regions due to absence of seismic excitation.

This test also suggests that the percentage of the false alarms by the TIMAP model is relatively large, which means that this model can be used as complementary of the D-AS model for which false alarms (from tests in random catalogues) are only 10%.

3. The Decelerating-Accelerating Seismic Strain (D-AS) Model

The D-AS model is defined by the power-law relation (1), as well as by other relations which have been derived by Papazachos et al. (2006). In the present work using additional recent global data these relations have been tested and in some cases were slightly modified. These refined relations are presented here for accelerating and decelerating preshock sequences.

3.1 Relations for accelerating preshocks

For accelerating preshocks the model is based on relation (1) and on the following semi-empirical constraints:

$$\log R = 0.42M - 0.30 \log s_a + 1.25, \quad \sigma = 0.15 \tag{5}$$

$$\log\left(t_c - t_{sa}\right) = 4.60 - 0.57 \log s_a, \quad \sigma = 0.10 \tag{6}$$

$$M = M_{13} + 0.60, \quad \sigma = 0.20 \tag{7}$$

where R (in km) is the radius of the circular (critical) region (or the radius of the equivalent circle in the case of an elliptical critical region), s_a (in Joule$^{1/2}$/yr.10^{4}km^2) is the rate of the long term Benioff strain per year and 10^{4}km^2 in the critical region, t_{sa} (in yrs) is the start time of the accelerating sequence, t_c is the origin time of the mainshock, M is the magnitude of the mainshock and M_{13} is the mean magnitude of the three largest preshocks (Papazachos et al., 2006).

In order to compare the obtained results regarding the R, M, t_{sa} values (estimated for each mainshock with the relations (5), (6), (7)), the probability of each obtained parameter was calculated. For this reason each model parameter was estimated with respect to its expected value, assuming that its deviations follow a Gaussian distribution. The average, P_a, of these probabilities is used as a measure of agreement of the determined parameters with those calculated by these global relations (Papazachos and Papazachos, 2001). Furthemore, for each point of the investigated area a "quality index", q_a, has been defined (Papazachos et al., 2002a) by the formula:

$$q_a = \frac{P_a}{mC} \tag{8}$$

where C is the curvature parameter (Bowman et al., 1998) and m is the parameter of relation (1). On the basis of a large sample of data concerning accelerating preshock sequences of mainshocks which

occurred in a variety of seismotectonic regimes and had magnitudes between 5.6 and 8.3 (Papazachos and Papazachos, 2000, 2001; Scordilis et al., 2004; Papazachos et al., 2005b) the following cut off values have been proposed:

$$C \leq 0.60, \quad P_a \geq 0.45, \quad 0.25 \leq m \leq 0.35, \quad q_a \geq 3.0 \tag{9}$$

Worldwide observations show that a mean value of m is 0.30, which is in agreement with theoretical considerations (e.g. Rundle et al., 1996; Ben-Zion et al., 1999). For these reasons, this value was adopted as fixed throughout the present work. The geographic point, Q, for which relations (9) are fulfilled and where the quality index, q_a, has its largest value is considered as the geometrical center of the critical region. The magnitude, M_{min}, of the smallest preshock of an accelerating preshock sequence for which relations (9) applies and q_a has its largest value is given by the relation:

$$M_{\min} = 0.46M + 1.91 \tag{10}$$

where M is the magnitude of the mainshock (Papazachos, 2003; Papazachos et al., 2005b). Thus, for mainshock magnitudes 6.0, 7.0 and 8.0 the corresponding minimum magnitudes of accelerating preshock sequences are 4.7, 5.1 and 5.6, respectively.

The accelerating seismic strain which complies with the constraints of relations (9) cannot be identified until a time, t_{ia}, before the generation of the mainshock, which is called "identification time". In practice, this is the earliest time for which the available data give a valid solution, assuming that the accelerating preshock sequence ends at the (true) origin time, t_c, of the mainshock. From global data concerning accelerating preshock sequences the following relation is derived:

$$\log\left(t_c - t_{ia}\right) = 2.51 - 0.30 \log s_a, \quad \sigma = 0.16 \tag{11}$$

Thus, for $logs_\alpha$ equal to 4.5 and 6.2, which correspond to the smallest and largest usually observed values of strain rate in our data-set, the identification time interval t_c-t_{ia} is equal to 14 years and 4 years, respectively.

The origin time, t_c, and the magnitude, M, of the mainshock depend also on the average origin time, t_a, and average magnitude, M_a, respectively, of the corresponding accelerating preshock sequence. Available data for estimating (predicting) t_c and M from equations (10) and (11) are those which concern accelerating preshocks which have occurred when such prediction is made, that is, a few years before the generation of the mainshock. Taking this into consideration and using the data of accelerating preshock sequences of the mainshokes listed on table (1) the following relations have been derived:

$$\log(t_c - t_a) = 3.11 - 0.36 \log s_a, \quad \sigma = 0.07 \tag{12}$$

$$M = 1.43M_a - 0.60, \qquad \sigma = 0.25 \tag{13}$$

where t_a and M_a is the average origin time and average magnitude, respectively, for the accelerating preshocks which occurred up to three years before the generation of the mainshock (Scordilis, 2010).

Accelerating preshocks are strong (see relation 10) and the largest of these can have magnitude larger than 6.0 and may cause damage. For this reason it is necessary to be able to estimate (predict) the largest accelerating preshock which occur, after the identification time which is given by relation (11) because an accelerating precursory sequence is recognizable after this time. Therefore, the time interval before the generation of the mainshock when the largest accelerating preshock is expected is given by relation (11). Thus, for the Aegean area, where $\log s_a \simeq 5.8$, this time interval is about 6 years. The

epicenter of the maximum accelerating preshock is in the region of the physical center, P_q, and in a maximum distance of 150km from the center. The magnitude, M_{ai}, of this shock is given by the relation;

$$M_{ai} = 0.68M + 1.60, \quad \sigma = 0.30 \tag{14}$$

where M is the mainshock magnitude, as it comes out from the data concerning accelerating preshock sequences of mainshocks listed on table (1). Thus, for mainshock magnitudes 6.5, 7.0, 7.5 and 8.0, the magnitudes of the largest accelerating preshocks are, on the average, 6.0, 6.4, 6.7 and 7.0, respectively.

3.2 Relations for decelerating preshocks

Decelerating seismic strain (Benioff strain) released by intermediate magnitude preshocks in the seismogenic region follows a power-law (relation 1 with m>1) and the relations:

$$\log a = 0.23M - 0.14 \log s_d + 1.40, \quad \sigma = 0.15 \tag{15}$$

$$\log\left(t_c - t_{sd}\right) = 2.95 - 0.31 \log s_d, \quad \sigma = 0.12 \tag{16}$$

where α (in km) is the radius of the circular seismogenic region, M is the magnitude of the mainshock, t_{sd} (in yrs) is the start time of the decelerating preshock sequence, and s_d (in Joule$^{1/2}$/yr.10^{4}km^2) is the long-term seismic strain rate (long-term seismicity) of the seismogenic region (Papazachos et al., 2006). A quality index, q_d, can be also defined by the relation:

$$q_d = \frac{P_d m}{C} \tag{17}$$

where P_d is defined for decelerating seismicity on the basis of quantities a, M, t_{sd} and relations (15, 16). The following cut-off values have been calculated by the use of data for decelerating preshock sequences of corresponding strong mainshocks which occurred in a variety of seismotectonic regimes (Papazachos *et al*., 2006):

$$C \le 0.60, \quad 2.5 \le m \le 3.5, \quad P_d \ge 0.45, \quad q_d \ge 3.0 \tag{18}$$

From relations (6) and (16) it is evident that the duration of accelerating and decelerating sequences is equal for strain rate $\log s_a = \log s_d = 6.35$. Since for most studied areas the strain rate is smaller, the accelerating sequence starts usually earlier than the corresponding decelerating sequence. Thus, for $\log s_d = \log s_a = 4.5$ (low seismicity areas) the duration of the decelerating and accelerating sequences is 36 and 108 years, respectively, while for $\log s_d = \log s_a = 6.2$ (very high seismicity regions) the two durations are almost equal (11 and 12 years, respectively).

Using global data it has been shown (Papazachos et al., 2006) that the minimum magnitude, M_{min}, of decelerating preshocks for which the best solution (smallest C value) is obtained, is given by the relation:

$$M_{\min} = 0.29M + 2.35 \tag{19}$$

where M is the magnitude of the mainshock. Thus, for mainshock magnitudes 6.0, 7.0 and 8.0 the corresponding values of M_{min} are 4.1, 4.4 and 4.7, respectively, which are much smaller than the corresponding minimum values (4.7, 5.1 and 5.6) for accelerating preshocks. It is interesting to note that decelerating seismicity which precedes strong mainshocks ($M \ge 6.0$) is also pronounced for intermediate magnitude ($M \ge 4.0$) preshocks. Data for such shocks are easily available.

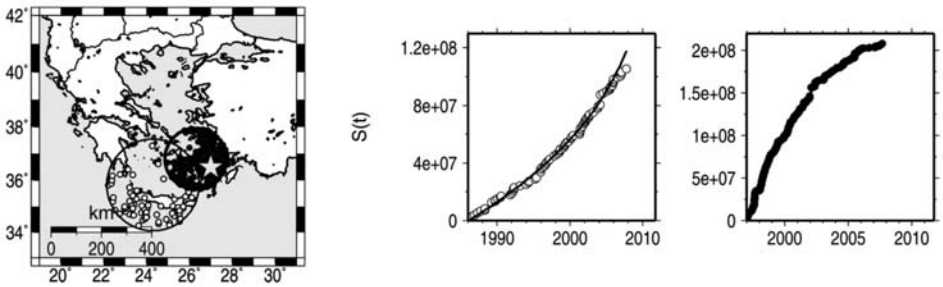

Fig. 2: Space and time variation of decelerating and accelerating preshocks observed (in 2007) before the generation of the strong (M = 6.4) 2008 earthquake near Rhodes island. Left: epicenters of decelerating preshocks (dots in the smaller of the two circles) and of accelerating preshocks (small white circles in the larger circle). The star is the predicted epicenter of the ensuing mainshock. Right: time variation of the Benioff strain, S(t), for decelerating preshocks (dots) and for accelerating preshocks (small white circles). The curves fit the data by a power-law (relation 1). The earthquake occurred (15 July 2008, M = 6.4, 36.0^{0}N, 27.9^{0}E, h = 60km) within the predicted time, magnitude and space windows (Papazachos and Karakaisis, 2008; Papazachos et al., 2009).

An "identification time" is also defined for each decelerating preshock sequence. Similarly to accelerating sequences, this is the earliest time, t_{id}, for which the available data fulfill constraints imposed by relations (18) and the end of the sequence coincides with the origin time of the mainshock. It has been shown that the logarithm of the difference between the origin time of the mainshock, t_c, and the identification time, t_{id}, of the decelerating preshock sequence scales negatively with the strain rate, s_d (Papazachos et al., 2005a). A revised form of this relation based on new additional data is:

$$\log\left(t_c - t_{id}\right) = 2.07 - 0.20 \log s_d, \quad \sigma = 0.15 \tag{20}$$

Thus, for logs_d equal to 4.5 and 6.2, t_c-t_{id} is equal to 15 years and 7 years, respectively.

From relations (11) and (20) it comes out that for $s_d = s_a$ the identification time of the decelerating sequence of a mainshock occurs earlier than the identification time of its accelerating sequence, although the accelerating sequence starts earlier (see relations 6 and 16).

The first part in the time variation of the Benioff strain graph appears to be almost linear for both accelerating and decelerating strain (see fig. 2) and the pattern can be identified after the time when it exceeds the background seismicity level. In a region of low background seismicity this "exceedance" and recognition will occur earlier than in a region of higher background seismicity, suggesting that the difference between the recognition time and the mainshock origin time decreases with increasing background seismicity. This explains why the difference between the origin time of the mainshock and the identification time, t_c-t_i, as well as between the origin time of the mainshock and the calculated start time, t_c-t_s, scale negatively with the long term strain rate, s, for precursory accelerating (relations 6, 11) and decelerating (relations 16, 20) seismic strain.

3.3 Additional predictive properties of the D-AS model

Relations presented in paragraphs (3.1) and (3.2) express predictive properties concerning the time and magnitude of an ensuing mainshock. In the present paragraph revised relations for the prediction of the mainshock epicenter are given. These relations concern the geographic distribution (with respect to the expected mainshock epicenter) of the quality indexes q_d and q_a (relations 8 and 17)

and of six distinct geographic points defined by the geographic distribution of decelerating and accelerating preshocks. An observed time variation of q_d and q_a, which is a qualitative predictive property of the model, is also presented. Uncertainties are also properties of the model and for this reason are examined in this work and are given in this section.

The curvature parameter, C, which qualifies the deviation of the Benioff strain from linearity, takes its smallest value at the center, F, of the decelerating preshocks, C_{df}, and at the center, Q, of the accelerating preshocks, C_{aq}. At other geographic points, including the epicenter, E, of the ensuing mainshock, the values of the curvature parameters are larger. Thus, the mean values of the curvature parameter for preshocks of the mainshocks listed on table (1) are $C_{df} = 0.32$, $C_{aq} = 0.42$ and the corresponding values for the mainshock epicenter are $C_{de} = 0.64$ and $C_{ae} = 0.71$. The larger values of the curvature parameters at the mainshock epicenter result in smaller values of the quality indexes (q_{de}, q_{ae}) at the actual mainshock epicenter with respect to the corresponding optimal values (q_{df}, q_{aq}) at the geometrical centers (F and Q). This is expressed by the following relation, which has been derived by using all available data for the preshock sequences of the mainshocks listed on table (1):

$$\frac{q_{de} + q_{ae}}{q_{df} + q_{aq}} = 0.45 \pm 0.13 \tag{21}$$

This relation applies at the vicinity of the mainshock epicenter and can be used as a constraint in estimating (predicting) this epicenter, as it is explained later.

The locations of three geographic points (F, P_f, V_f) defined by the space distribution of decelerating preshocks and of three corresponding points (Q, P_q, V_q) defined by the space distribution of accelerating preshocks can contribute to the prediction of the mainshock epicenter. F and Q are the geometrical centers of the circular regions of decelerating and accelerating preshocks. P_f and P_q are the physical centers of the two sequences where the density of decelerating and accelerating preshocks, respectively, is highest (Karakaisis et al., 2007). V_f and V_q correspond to the mean geographic center (mean latitude, mean longitude) of the epicenters of decelerating and accelerating preshocks, respectively. There are several ways in which these six points can be used to define the epicenter of the ensuing mainshock. A simple way is to separate the points into two groups and define the geographic mean (mean latitude and mean longitude) of each group. The first group is formed of the points (F, V_f, P_f) which are located in a relatively short distance from the mainshock epicenter and the distance of their geographic mean, D, from the mainshock epicenter, E, is:

$$\begin{aligned} (ED) &= 0.3(DA) + 35.0 \pm 40km, \quad for\ (DA) \le 250km \\ (ED) &= 120 \pm 50km, \qquad\qquad for\ (DA) > 250km \end{aligned} \tag{22}$$

The second group is formed of the three points (Q, V_q, P_q) which are located at relatively large distances from the mainshock epicenter and the distance of their geographic mean, A, from the mainshock epicenter is:

$$(EA) = 0.85(DA) + 50 \pm 80km \tag{23}$$

The available data for the preshock sequences considered in the present work show that the forty–six mainshock epicenters, E, have a tendency to delineate along the line AD and to distribute symmetrically with respect to this line. Thus, the mean distance, x, of E from DA is almost equal to zero

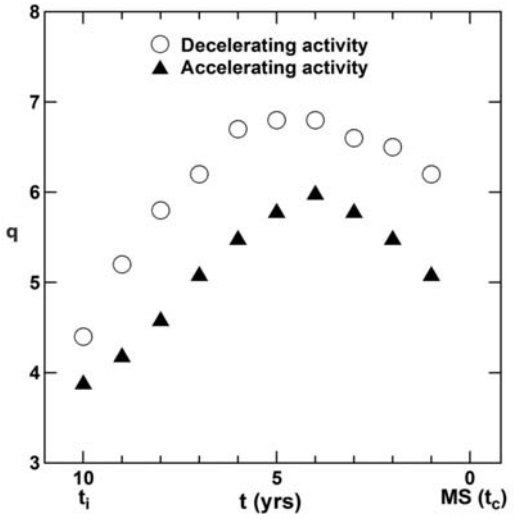

Fig. 3: Variation with the time, t (years), to the mainshock of the quality index, qd, for decelerating preshocks (open circles) and of the corresponding quality index, qa, for accelerating preshocks (black triangles) during the period between the identification time, ti, and the origin time, tc, of the mainshock.

(considering positive the distances of the points, E, which are in one side of DA and negative the distances of these points which are in the other side) with a standard deviation 80 km. That is,

$$x = 0 \pm 80km \tag{24}$$

The line DA intersects the circle (D, R = 120 km) in two points (D_1, D_2). D_1 is closer to the mainshock epicenter (from data of preshock sequences of mainshocks listed on table 1, $ED_1 = 80\pm40$ km and $ED_2 = 180\pm60$ km). Although D_1 is usually between D and A, we are not sure during the pre-mainshock period which of the two intersection points is closer to the epicenter of the ensuing mainshock. For this reason additional independent information is used, such as mean level of time dependent seismicity (e.g. the epicenter, E_t, defined by the TIMAP model in section 2.1) to resolve this ambiguity. Thus, if L_d is one of the points D_1 and D_2 which is in a higher seismicity level (closer to E_t), we can use the following relation as the fifth constraint for the location of the epicenter of the ensuing mainshock:

$$(EL_d) = 80 \pm 40km \tag{25}$$

The estimation (prediction) of the epicenter of an ensuing mainshock is based on constraints defined by relations (21, 22, 23, 24 and 25). That is, for each geographic point of a grid where the mainshock epicenter is expected (typically 2^ox2^o) a probability is calculated for each of these relations by assuming a normal (Gaussian) distribution for the observed deviations and the average of the five probabilities is considered as the representative value of probability for each grid point. The three points with the three highest such probabilities are defined and their geographic mean (mean latitude, mean longitude) is considered as the predicted epicenter. The retrospectively predicted parameters, t_c^*, $E^*(\phi,\lambda)$, M^* by the D-AS model of the 46 strong (M≥6.3) mainshocks are listed in table (1).

One should also consider variation with time to the mainshock of both quality indexes q_d and q_a. This variation is observed during the time period between the identification time (t_{id} or t_{ia}) and the origin time, t_c, of the mainshock (fig. 3). This allows a qualitative continuous inspection (monitoring) of the decelerating, $q_d = q_d(t)$, and accelerating, $q_a = q_a(t)$, preshock sequences with the time to the mainshock. Thus, both indexes increase from the corresponding identification times (t_{id}, t_{ia}) up to about the 60% of the time interval t_c-t_i and both decrease during the rest 40% of the time t_c-t_i. This suggests that during this last time interval before the mainshock, seismic excitation of preshocks declines in the broad (critical) region and is enhanced in the narrow (seismogenic) region.

Table 1. Observed origin time, t_c, epicenter coordinates, $E(\phi,\lambda)$, and moment magnitude, M, of the forty-six mainshocks and corresponding retrospectively predicted values, t^*_c, $E^*(\phi,\lambda)$, M^* for these parameters.

Area		t_c	$E(\phi,\lambda)$	M	t^*_c	$E^*(\phi,\lambda)$	M^*
Mediterranean	1	10.10.1980	36.2, 01.4	7.1	1981.9	36.2, -0.2	7.2
	2	23.11.1980	40.8, 15.3	6.9	1981.1	41.6, 14.0	6.8
	3	21.05.2003	36.9, 03.8	6.8	2001.6	36.0, 3.6	6.8
	4	24.02.2004	35.1, -04.0	6.4	2004.3	35.5, -4.9	6.3
Aegean	1	09.07.1980	39.3, 22.9	6.5	1980.4	39.0, 21.4	6.5
	2	24.02.1981	38.1, 23.0	6.7	1979.3	39.1, 24.1	6.8
	3	19.12.1981	39.0, 25.3	7.2	1982.6	38.4, 24.0	7.3
	4	17.01.1983	38.1, 20.2	7.0	1985.5	38.2, 20.4	6.7
	5	13.05.1995	40.2, 21.7	6.6	1994.3	39.9, 21.2	6.7
	6	13.10.1997	36.4, 22.2	6.4	1997.8	36.7, 22.3	6.4
	7	18.11.1997	37.5, 20.7	6.6	1997.8	36.9, 20.8	6.5
	8	26.07.2001	39.1, 24.4	6.4	2000.9	39.0, 23.6	6.6
	9	14.08.2003	38.7, 20.5	6.3	2003.8	38.7, 20.1	6.5
Anatolia	1	05.07.1983	40.2, 27.3	6.4	1983.3	39.9, 28.5	6.3
	2	13.03.1992	39.7, 39.6	6.6	1991.2	39.2, 38.4	6.5
	3	01.10.1995	38.1, 30.2	6.4	1996.7	39.1, 30.2	6.5
	4	09.10.1996	34.5, 32.1	6.8	1996.8	35.5, 32.0	7.0
	5	17.08.1999	40.8, 30.0	7.5	1993.3	39.6, 30.5	7.1
California	1	08.11.1980	41.1, -124.6	7.3	1981.1	41.6, -124.3	6.9
	2	02.05.1983	36.2, -120.3	6.4	1979.5	35.5, -119.1	6.4
	3	24.11.1987	33.0, -115.9	6.6	1986.7	33.2, -117.2	6.7
	4	18.10.1989	37.1, -121.9	6.9	1990.0	37.1, -122.3	6.8
	5	25.04.1992	40.3, -124.2	7.1	1991.9	39.5, -123.7	7.0
	6	28.06.1992	34.2, -116.4	7.3	1991.8	35.9, -116.2	7.4
	7	17.01.1994	34.2, -118.5	6.6	1993.4	34.5, -118.7	6.3
	8	22.12.2003	35.7, -121.1	6.5	2004.3	36.5, -120.3	6.4
Japan	1	12.07.1993	42.9, 139.2	7.7	1994.6	42.0, 139.5	7.8
	2	04.10.1994	43.7, 147.4	8.3	1995.6	43.3, 147.0	8.3
	3	16.01.1995	34.6, 135.0	7.0	1995.5	35.0, 134.7	7.2
	4	26.05.2003	38.8, 141.6	7.0	2003.0	39.3, 142.3	6.7
	5	25.09.2003	41.8, 143.9	8.3	2004.0	40.7, 144.0	8.3
	6	11.10.2003	37.8, 142.6	7.0	2003.8	36.6, 142.5	6.9
	7	05.09.2004	33.2, 137.1	7.4	2003.1	34.1, 137.5	7.6
	8	16.08.2005	38.3, 142.0	7.2	2004.6	39.4, 141.7	7.1
Central Asia	1	20.06.1990	37.0, 49.3	7.4	1990.6	36.1, 48.7	7.5
	2	19.08.1992	42.1, 73.6	7.2	1993.0	42.1, 72.7	7.1
	3	27.02.1997	30.0, 68.2	7.0	1998.0	30.3, 68.1	6.8
	4	10.05.1997	33.9, 59.8	7.3	1997.8	33.5, 59.8	7.3
	5	08.11.1997	35.1, 87.4	7.5	1996.1	34.6, 87.2	7.4
	6	06.12.2000	39.6, 54.8	7.0	2001.2	40.2, 53.5	7.2
	7	26.01.2001	23.4, 70.2	7.6	2001.2	23.1, 69.3	7.8
	8	14.11.2001	35.9, 90.5	7.8	2004.6	37.2, 91.1	7.7
	9	08.10.2005	34.5, 73.6	7.5	2007.2	35.7, 72.4	7.5
S. America	1	09.10.1995	19.1, -104.2	7.9	1991.9	19.8, -104.5	8.1
	2	13.01.2001	13.0, -88.7	7.7	1998.6	13.2, -88.3	7.9
	3	23.06.2001	-16.3, -73.6	8.3	2001.6	16.5, -74.6	8.2

To define the model uncertainties of the D-AS model with respect to: the origin time, magnitude and epicenter of an ensuing mainshock, a backward test was performed by applying the model to the already occurred preshock sequences of the 46 strong mainshocks listed in table (1). This postdiction resulted in uncertainties: $\pm$2.5 years for the origin time of the mainshock, $\pm$0.4 for its predicted magnitude and $\leq$150km for its epicenter with a probability 90%. Since the probability of the D-AS model for false alarms is of the order of 10%, the total probability for these time, magnitude and space windows is reduced to 80%. This result confirms previous similar results (Papazachos et al., 2006).

When the epicenter, E_t, estimated by the TIMAP model is known (see section 2.1) the finally predicted by both models epicenter is based on relations (21), (22), (23), (24) and (25) and on the relation:

$$(EE_t) = 90 \pm 40km \tag{26}$$

Also, the finally adopted magnitude is the average of the three magnitudes defined by the D-AS model and of the M_t magnitude defined by the TIMAP model. The 2σ uncertainties when estimations are based on both models are: $\pm$2.5 years for the origin time, $\leq$120 km for the epicenter and $\pm$0.4 for the magnitude of the ensuing mainshock with a probability about 80%.

3.4 Physical explanation of accelerating and decelerating precursory strain

Decelerating and accelerating precursory seismicity, the relative relations and values of parameters are mainly results of seismological observations. These empirical results, however, need physical explanation to support their scientific validity. Several such attempts have been already made but there are usually more than one proposals for possible physical models and interpretations. The results of the present work allow the resolutions of such ambiguities.

3.4.1 Physical explanation of accelerating strain

Accelerating precursory Benioff strain has been physically explained by principles of the critical point dynamics, that is, by considering the process of generation of the moderate magnitude accelerating preshocks as a critical phenomenon, culminating in a large event (mainshock) considered as a critical point (Allègre and Mouël, 1994; Sornette and Sammis, 1995; Rundle et al., 2003). We are presenting in this section additional observational information which supports critical triggering of mainshocks by accelerating preshocks and that this triggering is associated with quasi–static stress changes.

Accelerating strain observed for the forty six accelerating preshock sequences considered in the present work occurred at relatively large and much variable distances from the mainshock epicenter ($EQ = 270\pm120$ km). For this reason it is not possible that pre-mainshock static stress changes trigger accelerating preshocks or that static stress change produced by such preshocks trigger the mainshock.

Therefore, critical triggering of the mainshock by accelerating preshocks through a physical process with gradual stress changes and viscous relaxation of the lower crust and upper mantle can explain observed properties (long distances and delay times) of accelerating preshocks. That is, quasi–static stress change explains contribution to triggering of the mainshock by accelerating preshocks because such stress change decays slowly with distance, which means that their triggering potential extends to greater distances than static stress change and because the relatively low speed of viscoelastic propagation results in delayed triggering.

Critical triggering predicts increase of the maximum magnitude of accelerating preshocks with the time to the mainshock. To test it, we divided the total duration of each of the examined 46 acceler-

ating preshock sequences into ten equal time intervals and for each interval the difference of the maximum preshock from the corresponding mainshock was calculated. Then, the mean of these 46 differences for each interval was calculated and the time variation of this mean difference was defined. It was observed that this difference decreases with the time to the mainshock, which means that the magnitude of the largest accelerating preshock increases with the time to the mainshock. This observational result shows that accelerating seismic strain is mainly due to an increase of the magnitude of accelerating preshocks and supports critical triggering of mainsocks by accelerating preshocks. In the same way it has been shown that the frequency (number) of accelerating preshocks also increases with the time to the mainshock.

In the accelerating preshock sequences considered in the present work, there are several cases where a critical region overlaps partly with another which means that an accelerating shock can be preshock of more than one ensuing mainshocks. This observation supports the idea that accelerating preshocks affect the generation of mainshocks by critical triggering.

A power- law for the time variation of accelerating preshock strain, such as relation (1), which has been derived on the basis of damage mechanics theory (Bufe and Varnes, 1993), is also expected if seismic cycle is modeled as a critical phenomenon (Sornette and Sammis, 1995; Saleur at al., 1996). Furthermore, the mean of the observed values of m for this relation is equal to 0.3 (Papazachos and Papazachos, 2001; Ben-Zion and Lyakovsky, 2002) in agreement with values of this parameter determined theoretically on the basis of the critical point dynamics (Rundle et al., 1996; Ben-Zion et al., 1999).

3.4.2 Physical explanation of decelerating strain

Decelerating seismic strain is composed of two main phases. The first is a phase of excitational seismic strain which ends at the identification time (t_{id} in relation 20). The second phase follows and covers a period of decrease (quiescence) for the seismic strain.

Relations (6) and (16) show that increase of precursory strain in the critical region starts before the increase of precursory strain in the seismogenic region. This observation suggests that the first (excitational) phase of precursory strain in the seismogenic region can be a result of contribution of critical (quasi–static) triggering in addition to tectonic stressing. It has been further examined: what is the cause of the following deceleration of seismic strain in the seismogenic region and how the mainshock is triggered by preshocks which occur in the seismogenic region during the phase of decelerating strain.

Decelerating preshocks are generated close to the mainshock epicenter ($FE = 130 \pm 40$ km) and relatively shortly before the mainshock. These observations indicate that changes of static (Coulomb) stress caused by preshocks in the seismogenic region during the decelerating phase contribute to triggering of the mainshock. It must be also taken into account that decelerating preshocks considered in the present work have magnitudes larger than a certain value (see relation 19), which means that there is a finite number of faults where shocks of a decelerating preshock sequences occur.

A frictional stability model (Gomberg et al., 1998) where a seismic fault obeys rate–and–state frictional constitutive relations (Dieterich, 1992, 1994) can explain seismic quiescence that follows a seismic excitation. Thus, this model predicts that, if triggering results from advancing the failure time of inevitable earthquakes and if the population of the available faults is finite, a static load results in seismic excitation followed by seismic quiescence, as it occurs with decelerating preshocks considered in the present work. That is, the seismic excitation in a finite number of faults of the seismogenic region leaves fewer faults available for failure and thus quiescence follows the seismic excitation.

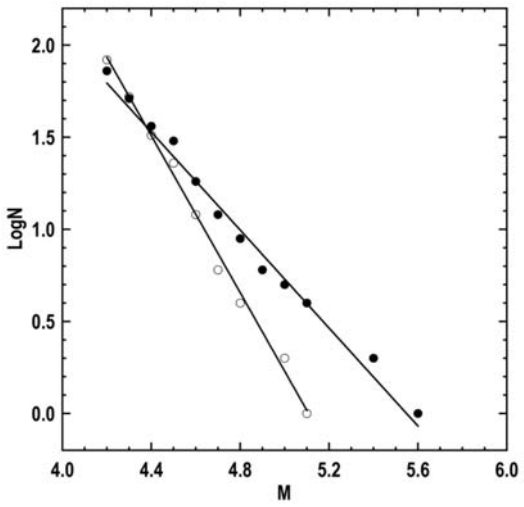

Fig. 4: Cumulative distribution of preshocks in the narrow (seismogenic) region of the mainshock with M = 6.2 which occurred on 6 November 1992 in eastern Aegean (38.1^{0}N, 27.0^{0}E). Dots refer to preshocks which occurred in the seismogenic region before the identification time, when the slope is b = 1.3. Small open circles refer to preshocks occurred in the same region after the identification time when b = 2.1.

Decelerating preshocks are relatively small (see relation 19) and their individual effect on static stress changes is also small because this change increases with the magnitude, M, of the triggering earthquake as $\sim 10^{aM}$. It has been shown, however, that if triggering earthquakes follow the Gutenberg–Richter law with $b>a(= D/2$, where D is the fractal dimension), small earthquakes dominate in stress transfer and earthquake triggering because their high frequency overcomes their small individual triggering potential (Helmstetter, 2003; Helmstetter et al., 2005). For earthquake triggering due to static stress we have $D\sim 2$, which is also interpreted as the fractal dimension of an active fault network. Therefore, seismic sequences with $b>1$ have an increased triggering potential. Such seismic sequences can also trigger strong mainshocks because in static triggering the magnitude of the triggered earthquake is independent of the magnitude of the triggering earthquake (Helmstetter, 2003).

Therefore, it is of importance to calculate the b value of preshocks in the seismogenic region during the time of decelerating strain (second phase) and compare b values with $D/2$. For this purpose, we considered the decelerating preshock sequences of all 12 mainshocks which occurred in the Aegean between 1980 and 2004 and have magnitudes $M \geq 6.1$ (Papazachos et al., 2006). The b value has been calculated by least-squares for the first phase of each decelerating sequence (excitational phase), as well as for its second (later) phase. For the first twelve phases b values between 0.8 and 1.9 have been calculated with a mean and corresponding standard deviation 1.3 ± 0.3. For the twelve late phases b values between 1.1 and 2.1 have been calculated with a mean and corresponding standards deviation 1.6 ± 0.3. That is, all late decelerating preshock sequences, which occurred shortly before the corresponding mainshocks, have high b values and their triggering potential is high. It is, therefore, reasonable to assume that small preshocks which occur in the seismogenic region during the second phase contribute to triggering of the mainshock by increasing static stress.

Figure (4) shows a representative case of variation of the cumulative frequency, N, of decelerating preshocks with their magnitude, M, which started on 4.1.1982 and lasted till the generation of their mainshock (6.11.1992, M = 6.2, 38.1^{o}N, 27.0^{o}E, east Aegean). The first (excitational) phase lasted till 27.10.1984 (~2.7 years) and the frequency distribution (dots in fig. 4) of preshocks of this phase is fitted (in the least-square sense) by the relation:

$$\log N = 7.4 - 1.3M \tag{27}$$

with a high correlation coefficient (r = -0.99). The second (quiescence) phase lasted till the generation of the mainshock (~8.0 years) and the frequency distribution (small open circles in fig. 4) of preshocks of this phase is fitted by the relation:

$$\log N = 10.9 - 2.1M \tag{28}$$

with also a high correlation coefficient (r = -0.99). It is observed (fig. 4, relations 27, 28) that for intermediate magnitude preshocks (4.4–5.6) the frequency in the seismogenic region is high during the excitational phase and is much reduced during the quiescence phase. This explains the corresponding reduction of the calculated Benioff strain and its deceleration with the time to the mainshock. It is also observed that the frequency of the small preshocks in the seismogenic region is high during the second period of the sequence, as it is shown by the increase of the b value, that is, the frequency of small (M<4.4) preshocks is high in the seismogenic region during the whole preshock time period (t_c-t_{sd}).

3.5 Successful predictions by the D-AS model

In addition to backward tests of the D-AS model to estimate its uncertainties, forward tests have been also performed by attempting prediction of future strong (M≥6.3) earthquakes to evaluate its prediction ability in a more objective way. By such forward tests, two strong earthquakes which occurred recently (2006, 2008) in the Aegean area have been successfully predicted. The first of these mainshocks occurred on 8 January 2006 in southwestern Aegean, near the Cythera island, with epicenter coordinates ($\phi = 36.2^0$N, $\lambda = 23.4^0$E), focal depth h = 65km and moment magnitude M = 6.9. The second earthquake occurred on 15 July 2008 in southeastern Aegean, near the Rhodes island ($\phi = 36.0^0$N, $\lambda = 27.9^0$E, h = 60km), with moment magnitude M = 6.4.

Identification of an accelerating pattern of intermediate magnitude preshocks in southwestern Aegean was initially made by using data up to 1 July 2000 and resulted in the estimation (prediction) of epicenter coordinates $\phi = 36.4^0$N, $\lambda = 23.0^0$E, h≤100km, M = 6.8 and time window 2001.3-2004.3 (Papazachos et al., 2002a). Estimation was repeated by the use of additional data collected during the next two years and the prediction based on data up to 1 July 2002 was: epicenter coordinates ($\phi = 36.5^0$N, $\lambda = 23.7^0$E with uncertainty ≤120km), h≤100km, M = 6.9±0.5, origin time t_c = 2006.4±2.0years. That is, the earthquake occurred within the predicted space, magnitude and time windows with a high probability (~80%), while the probability for random occurrence is about 4% (Papazachos et al., 2002b, 2007).

Identification of a decelerating and an accelerating pattern of intermediate magnitude preshocks in southeastern Aegean was made by using data up to 1 October 2007 and resulted in the estimation (prediction) of epicenter coordinates: $\phi = 36.5^0$N, $\lambda = 27.0^0$E with an uncertainty ≤150km, focal depth h≤100km, magnitude $M = 6.5\pm0.4$ and time $t_c = 2010.5\pm2.5$years (Papazachos and Karakaisis, 2008; Papazachos et al., 2009), with a probability of 80% while the probability for random occurrence of the earthquake in these space, magnitude and time windows is much smaller (~36%).

4. Conclusions and Discussion

1. Mainshocks generated by tectonic loading in a network of main faults located in a zone of lithospheric interaction have a quasi-periodic behavior. This is the basic property of the Time and Magnitude Predictable (TIMAP) regional model which is expressed by relation (2). This property, combined with the observation that the ratio T/T_t of the observed repeat times, T, to that, T_t, given by relation (2) follows a lognormal distribution, allows the estimation of the probability for the occurrence of a mainshock in this predefined mainshocks' regions during the next Δt years.

2. The second property of the TIMAP model is expressed by relation (3) which allows the estimation (prediction) of the magnitude, M_f, of the following mainshock in a faults' region. An interesting property expressed by this relation is that the magnitude, M_f, of the ensuing mainshock in the region is negatively related with the magnitude, M_p, of the previous mainshock of the region. It means that the break of a large fault in the region at the start of a period is followed by the break of a smaller fault in this region at the end of the period and vice versa.

3. A backward test of the TIMAP model by attempting retrospective prediction (postdiction) of the last strong ($M \geq 6.0$) mainshock in 86 circular faults' regions of the Aegean area during a period Δt = 10 years, which starts 2 years before the mainshock, gave reasonable results. Also, the mean difference of the observed magnitude and the estimated (predicted) magnitude, M_t (see section 2.1), is almost zero with a standard deviation equal to 0.21.

The Decelerating – Accelerating Strain (D-AS) model, which has been further developed in the present paper by the use of recent global data, has characteristics and predictive properties which are summarized and discussed in the following paragraphs.

4. The D–AS model is based on precursory seismicity change formed of two patterns. The first one is a precursory accelerating generation of the intermediate magnitude shocks which has been observed in a broad region (called in the present work "critical region"). The second pattern is a precursory decelerating generation of intermediate magnitude shocks which is observed in the narrow focal region (called in the present work "seismogenic region"). Both patterns are results of observations made by many workers, by several techniques and in various seismotectonic regimes (see section 3). For this reason these two patterns can be considered as distinct precursory seismicity patterns.

5. The model has been developed on the basis of precursory seismicity of many complete samples of mainshocks which occurred in the Aegean area, western Mediterranean, Anatolia, California, Japan, Central Asia and in south and Central America. The D–AS model is also tested in the present work by recent data concerning preshock sequences of 46 mainshocks which form 7 complete samples and occurred in corresponding seven seismotectonic regimes (see table 1). The validity of the model for all preshock sequences of so many mainshocks which form complete samples and occurred in corresponding different seismotectonic regimes is a very strong evidence that these two seismicity patterns precede systematically strong ($M \geq 6.3$) mainshocks and the D–AS model is of general validity.

6. The D–AS model has been also tested by synthetic but realistic catalogues which show that the probability for false alarms is low (~10%). This is not surprising because the model is based on many properties of a large number of real preshock sequences that put important observational constraints which cannot be easily fulfilled randomly.

7. Although the relations and parameters of the model are based mainly on observations, there are several of them which have been derived theoretically or have been interpreted physically. Thus, relation (1) has been derived on the basis of principles of damage mechanics, as well as on the basis of the critical point dynamics. The mean value of m (= 0.3) of relation (1) which has been calculated observationally by several investigators has been also derived theoretically. Relation (5) and the values of its scaling coefficients (0.42, –0.30) which are based on observations have been also derived theoretically. Relations (11, 20) which predict smaller identification period (t_c–t_{ia}, t_c–t_{id}) for regions of higher seismicity are physically explained because Benioff strain graphs cut high levels of background seismicity closer to the origin time of the mainshock than low levels of background seismicity.

8. Most of the relative published works consider accelerating precursory strain as a result of criticality and that the generation of the mainshocks is due to stress change by critical triggering. Observations made in the present work on 46 accelerating preshock sequences support this idea because the maximum magnitude of preshocks increases with the time to the mainshock as it is predicted by the

critical point theory. Evidence is also presented in the present work that during this physical process stress is transferred in a quasi–static mode and contributes to triggering of the mainshock. The total duration, t_c–t_{sa}, of an accelerating seismic sequence includes two phases. During the first phase, which lasts from the start (t_{sa}) of the sequence till its identification time (t_{ia}), the time variation of the cumulative Benioff strain is almost linear (see fig. 2). During the second phase, which lasts from the identification till the origin time, t_c, of the mainshock, the Benioff strain is accelerating. In most of the sequences the second phase starts with a period of accelerating strain which covers about 60% of the phase (increase of q_a in fig. 3) followed by a period of strain decrease (decrease of q_a in fig. 3), which lasts till the mainshock and is probably due to a return of seismicity to its background level.

9. Precursory seismic quiescence near the focus of many ensuing mainshocks has been observed by several seismologists. In most of these cases it concerns decrease of the frequency of small earthquakes and in others decrease of seismic deformation. By using data concerning the 46 decelerating preshock sequences studied in the present work we have shown that it is the frequency of intermediate magnitude preshocks (M>4.0) in the seismogenic region which increases originally (excitational phase) and then decreases (seismic quiescence phase), that causes corresponding changes in the Benioff strain. The first phase (excitational) which lasts from the start time, t_{sd}, of the sequence till the identification time, t_{id}, is attributed to critical triggering and tectonic stressing. In the second phase, which lasts between t_{id} and t_c, the Benioff strain declines due to decrease of the frequency of the intermediate magnitude preshocks, while the frequency of small shocks (M<4.0) continues to be high during this phase as it comes out from the observed high b value. Decrease of the frequency of the intermediate magnitude preshocks in the seismogenic region (and corresponding quiescence of strain) in the second phase is attributed to the fact that many faults of the seismogenic region were broken during the first (excitational) phase and few left available for failure during the second phase. The triggering ability of the small shocks which occur in the seismogenic region during the second phase is high due to their very large number (b>D/2). This observation and the fact that these small earthquakes occur close to the mainshock (in space and time) suggest that their generation transfer static stress which contributes to triggering of the mainshock. Usually, the second phase is formed of two periods. During the first period, which covers about 60% of the total duration of the phase, the Benioff strain decelerates (increase of q_d in fig. 3). During the second period the Benioff strain increases (decrease of q_d in fig. 3), which means a return of seismicity in the seismogenic region to its background level.

10. Neither the center of the seismogenic region (point F of decelerating preshocks) nor the center of the critical region (point Q of accelerating preshocks) coincides with the mainshock epicenter. However, the center, F, of the seismogenic region is at a relatively short distance from the mainshock epicenter and thus the generation of a very large number of small preshocks (indicated by an increase of the b value) is able to increase static stress and contribute to the triggering of the mainshock. On the contrary the center, Q, of the critical region is at large and variable distances from the mainshock epicenter but due to the large magnitudes of accelerating preshocks (see relation 10) and to the increase of their magnitude and of their frequency with the time to the mainshock, accelerating preshocks can also contribute to the triggering of the mainshock but by quasi–static stress transfer.

11. Another strong evidence for the scientific validity of the D–AS model is that properties of this model have been already applied for intermediate–term successful prediction of two recent strong earthquakes in the Aegean area. The first of these earthquakes, which occurred on 8 January 2006 near the Cythera island (southwest Aegean) with M = 6.9, has been successfully predicted (time, space and magnitude within the predicted windows) in 2002 by the use of data concerning precursory accelerating strain (Papazachos et al., 2002b). The second earthquake, which occurred on 15 July 2008 near Rhodos island (southeast Aegean) with M = 6.4 has been also successfully predicted (on April 2008) by application of the D–AS model (Papazachos and Karakaisis, 2008; Papazachos et al., 2009).

12. Estimation (prediction) of the origin time, t_c, magnitude, M, and epicenter coordinates, $E(\phi, \lambda)$, of an ensuing mainshock is based on empirical relations which express predictive properties of the D–AS model. Thus, the origin time, t_c, is calculated by relations (6), (12) and (16), the magnitude, M, by relations (5), (13) and (15) and the geographic coordinates of the epicenter of the mainshock by constraints put by relations (21), (22), (23), (24) and (25). Retrospective "predictions" (postdictions) of the 46 mainshocks listed on table (1) and comparison of the predicted values with the observed ones confirm that uncertainties are: $\pm$2.5 years for the origin time, $\pm$0.4 for the magnitude and less than 150km for the epicenter, with a probability 80% if we take into consideration false alarms estimated by application of the model in random but realistic catalogues. The error in the epicenter is reduced to $\leq$120 km if results of the TIMAP model are also considered.

5. References

Allègre, C.J. and Le Mouël, J.L., 1994. Introduction to scaling techniques in brittle failure of rocks. *Phys. Earth Planet. Inter.* 87, 85-93.

Ben-Zion, Y., Dahmen, K., Lyakhovsky,V., Ertas, D. and A. Agnon, 1999. Self-driven mode switching of earthquake activity on a fault system. *Earth Planet. Science Lett.* 172, 11-21.

Ben-Zion, Y. and V. Lyakhovsky, 2002. Accelerated seismic release and related aspects of seismicity patterns on earthquake faults. *Pure appl. Geoph.* 159, 2385-2412.

Bowman, D.D., Quillon, G., Sammis, C.G., Sornette, A. and D. Sornette, 1998. An observational test of the critical earthquake concept. *J. Geophys. Res.* 103, 24359-24372.

Brehm, D.J., and L.W. Braile, 1998. Intermediate-term earthquake prediction using precursory events in the New Madrid seismic zone. *Bull. Seism. Soc. Am.* 103, 24359-24372.

Brehm, D.J., and L.W. Braile, 1999. Refinement of the Modified Time-to-failure Method for Intermediate-term Earthquake Prediction. *J. Seismology* 3, 121-138.

Bufe, C.G., and D.J. Varnes, 1993. Predictive modeling of seismic cycle of the Great San Francisco Bay Region. *J.Geophys. Res.* 98, 9871-9883.

Das, S. and C. Scholz, 1981. Off-fault aftershock clusters caused by shear stress increase. *J. Geophys. Res.*, 71, 1669-1675.

Dieterich, J.H., 1992. Earthquake nucleation on faults with rate and state dependent strength, *in Earthquake Source Physics and Earthquake Precursors, edited by T. Mikumo et al., Elsevier, NY,* 115-134.

Dieterich, J.H., 1994. A constitutive law for rate on earthquake prediction and its application to earthquake clustering. *J. Geophys. Res.*, 99, 2601-2618.

Evison, F.F., and D.A. Rhoades, 1997. The precursory earthquake swarm in New Zealand. *N.Z.J. Geol. Geophys.* 40, 537-547.

Evison, F.F., 2001. Long-range synoptic earthquake forecasting: an aim for the millennium. *Tectonophysics* 333, 207-215.

Fedotov, S.A., 1965. Regularities of the distribution of strong earthquakes in Kamchatka, the Kurile Islands and Northeastern Japan (in Russian), *Tr. Inst. Fiz. Zemli, Akad. Naua SSSR,* 36, 66-93.

Freed, A.M., 2005. Earthquake triggering by static, dynamic and postseismic stress transfer. *Ann. Rev. Earth Planet. Sci.*, 33, 335-367.

Gomberg, J., Beeler, N.M., Blanpied, M.L. and Bodin, P., 1998. Earthquake triggering by transient and static deformations. *J. Geophys. Res.*, 103, 24411-24426.

Helmstetter, A., 2003. Is earthquake triggering driven by small earthquakes?. *Physical Review Letters*, 91, 058501-4.

Helmstetter, A., Kagan, Y.Y. and Jackson, D.D., 2005. Importance of small earthquakes for stress transfers and earthquake triggering. *J. Geophys. Res.*, 110, B05508, doi: 10.1029/2004JB003286.

Hill, D.P. and Prejean, S.G., 2006. Dynamic triggering. *Treatise on Geophysics*, 4, 1-52.

Jaumé, S.C. and L.R., Sykes 1999. Evolving towards a critical point: a review of accelerating seismic moment/energy release rate prior to large and great earthquakes. *Pure Appl. Geophys*. 155, 279-306.

Karakaisis, G.F., Papazachos, C.B., Panagiotopoulos, D.G., Scordilis, E.M. and B.C. Papazachos, 2007. Space distribution of preshocks. *Boll. Geof. Teor. Aplic*. 48, 371-383.

Karakaisis, G.F., Papazachos, C.B. and E.M. Scordilis, 2010. Seismic sources and main seismic faults in the Aegean and surrounding area. *Bull. Geol. Soc. Greece*, (submitted).

Kato, N., Ohtake, M. and T. Hirasawa, 1997. Possible mechanism of precursory seismic quiescence: Regional stress relaxation due to preseismic sliding. *Pure Appl. Geophys*. 150, 249-267.

Kilb, D., Gomberg, J. and Bodin, P., 2002. Aftershocks triggering by complete Coulomb stress changes. *J. Geophys. Res*., 107, doi: 10.1029/2001JB000202.

King, G.C.P. and M. Cocco, 2001. Fault interactions by elastic stress changes: new clues from earthquake sequences. *Advances in Geophysics*, 44, 1-38.

Knopoff, L., T.Levshina, V.J. Keillis-Borok and C. Mattoni, 1996. Increased long-rang intermediate-magnitude earthquake activity prior to strong earthquakes in California. *J.Geophys. Res*. 101, 5779-5796.

Mignan, A., D.D. Bowman, and G.C. King, 2006. An observational test of the origin of accelerating moment release before large earthquakes. *J. Geophys. Res*. Doi:10.1029/2006JB004374.

Mogi, K., 1969. Some features of the recent seismic activity in and near Japan.II. Activity before and after great earthquakes. *Bull. Earthquake Res, Inst. Univ.Tokyo* 47, 395-417.

Papazachos, B.C., 1989. A time predictable model for earthquakes in Greece. *Bull. Seism. Soc. Am*., 79, 77-84.

Papazachos, B.C. and Ch.A. Papaioannou, 1993. Long term earthquake prediction in the Aegean area based on the time and magnitude predictable model. *Pure Appl. Geophys*., 140, 593-612.

Papazachos, B.C., Papadimitriou, E.E., Karakaisis, G.F. and Panagiotopoulos, D.G., 1997. Long-term earthquake prediction in the Circum-Pacific convergent belt. *Pure Appl. Geophys*., 149, 173-217.

Papazachos, B.C. and C.B. Papazachos, 2000. Accelerated preshock deformation of broad regions in the Aegean area. *Pure Appl. Geophys*. 157, 1663-1681.

Papazachos, B.C., Karakaisis, G.F., Papazachos, C.B., Scordilis, E.M. and A.S. Savvaidis, 2002b. Space and time variation of seismicity in the region of Greece. *Final report to the Greek Earthquake Planning and Protection Organization (OASP) under project 20242, Aristotle University of Thessaloniki, Research Committee (3 December 2002)*, 21pp.

Papazachos, B.C. and Papazachou, C.B., 2003. The earthquakes of Greece. *"Ziti Publications, Thessaloniki"*, 273pp.

Papazachos, B.C., Karakaisis, G.F., Papazachos, C.B. and E.M. Scordilis, 2007. Evaluation of the results for an intermediate term prediction of the 8 January 2006 M_W = 6.9 Cythera earthquake in southern Aegean. *Bull. Seism. Soc. Am*. 97, 1B, 347-352.

Papazachos, B.C. and G.F. Karakaisis, 2008. Present space-time evolution of seismicity in the region of Greece. *Official Report to the Minister of Public Works of Greece*, 7pp, 30 June 2008.

Papazachos, B.C., Comninakis, P.E., Scordilis, E.M., Karakaisis, G.F. and Papazachos, C.B., 2008. A catalogue of earthquakes in Mediterranean and surrounding area for the period 1901-2008, *Publ. Geoph. Laboratory, University of Thessaloniki*.

Papazachos, B.C., Karakaisis, G.F., Papazachos, C.B., Panagiotopoulos, D.G. and E.M. Scordilis, 2009. A forward test of the Decelerating-Accelerating Seismic Strain Model in the Mediterranean. *Boll. Geofis. Teor. Applic*.,50, 3, 235-254.

Papazachos, C.B., 2003. Minimum preshock magnitude in critical regions of accelerating seismic crustal deformation. *Boll. Geof.Teor. Aplic*. 44, 103-113.

Papazachos, C.B. and B.C. Papazachos, 2001. Precursory accelerating Benioff strain in the Aegean area. *Ann. Geofisica* 144, 461-474.

Papazachos, C.B., Karakaisis, G.F., Savaidis, A.S., and B.C. Papazachos, 2002a. Accelerating seismic crustal deformation in the southern Aegean area. *Bull. Seismol. Soc. Am.* 92, 570-580.

Papazachos, C.B., Scordilis, E.M., Karakaisis, G.F. and B.C. Papazachos, 2005a. Decelerating preshock seismic deformation in fault regions during critical periods. *Bull. Geol. Soc. Greece* 36, 1491-1498.

Papazachos, C.B., Karakaisis, G.F., Scordilis, E.M. and B.C. Papazachos, 2005b. Global observational properties of the critical earthquake model. *Bull. Seismol. Soc. Am.* 95, 1841-1855.

Papazachos, C.B., Karakaisis, G.F., Scordilis, E.M. and B.C. Papazachos, 2006. New observational information on the precursory accelerating and decelerating strain energy release. *Tectonophysics* 423, 83-96.

Pollitz, F.F. and Sacks, I.S., 2002. Stress triggering of the 1999 Hector Mine earthquake by transient deformation following the 1992 Landers earthquake. *Bull. Seism. Soc. Am.*, 92, 4, 1487-1496.

Robinson, R., 2000. A test of the precursory accelerating moment release model on some recent New Zealand earthquakes. *Geoph. J. Int.* 140, 568-576.

Rhoades, D.A. and F.F. Evison, 1993. Long-range earthquake forecasting based on a single predictor. *Geophys. J. Int.* 113, 371-381.

Rundle, J.B., Klein, W. and S. Gross, 1996. Dynamics of a traveling density wave model of earthquakes. *Phys. Rev. Lett.* 76, 4285-4288.

Rundle, J.B., Turcotte, D.L., Shecherbakov, R., Klein, W. and C. Sammis, 2003. Statistical physics approach to understanding the multiscale dynamics of earthquake fault systems. *Rev. Geophys.*, 41, 5/1-5/30.

Saleur, H., Sammis, C.G. and D. Sornette, 1996. Discrete scale invariance, complex fractal dimensions and long-periodic fluctuation in seismicity. *J. Geophy. Res.* 101, 17661-17678.

Scordilis, E.M., 2010. Correlations of the Mean Time and Mean Magnitude of Accelerating Preshocks with the Origin Time and Magnitude of the Mainshock. *Bull. Geo. Soc. Greece*, (submitted).

Scordilis,E.M., Papazachos,C.B., Karakaisis,G.F. and V.G. Karakostas, 2004. Accelerating seismic crustal deformation before strong mainshocks in Adriatic and its importance for earthquake prediction. *J. Seismology* 8, 57-70.

Shimazaki, K. and Nakata, T., 1980. Time predictable recurrence model for large earthquakes. *Geophys. Res. Lett.*, 7, 279-282.

Sornette, D., and C.G. Sammis, 1995. Complex critical exponents from renormalization group theory of earthquakes: implications for earthquake predictions. *J.Phys. I.France* 5, 607-619.

Steacy, S., Gomberg, J. and Cocco, M., 2005. Introduction to special section: Stress transfer, earthquake triggering and time-dependent seismic hazard. *J. Geophys. Res.,* 110, doi: 10.1029/2005JB003692.

Sykes, L.R., and S.C. Jaumé, 1990. Seismic activity on neighboring faults as a long term precursor to large earthquakes in the San Francisco Bay area. *Nature* 348, 595-599.

Tocher, D., 1959. Seismic history of the San Francisco bay region. *Calif. Div. Mines Spec. Rep.* 57, 39-48.

Tzanis, A., F. Vallianatos, and K. Makropoulos, 2000. Seismic and electric precursors to the 17-1-1983, M7 Kefallinia earthquake, Greece: signatures of a SOC system. *Phys. Chem. Earth* 25, 281-287.

Tzanis, A., and K. Makropoulos, 2002. Did the 7/9/1999, m5.9, Athens earthquake came with a warning?. *Natural Hazards* 27, 85-103.

Varnes, D.J., 1989. Predicting earthquakes by analyzing accelerating precursory seismic activity. *Pure Appl. Geophys.* 130, 661-686.

Wyss, M., 1997. Cannot earthquakes be predicted?. *Science* 278, 487-488.

Wyss, M., Klein, F. and A.C. Johnston, 1981. Precursors of the Kalapana M = 7.2 earthquake. *J. Geophys. Res.* 86, 3881-3900.